

The Twelfth East Asia-Pacific Conference on Structural Engineering and Construction

## Seismic Performance of Continuous Girder Bridges Using Cable-sliding Friction Aseismic Bearing

Zhenghua Wei<sup>1ab</sup>, Wancheng Yuan<sup>2</sup>, Pak-chiu Cheung<sup>3</sup>, Xinjian Cao<sup>4</sup>, Zhaojun Rong<sup>5</sup>

<sup>1</sup> State Key Laboratory of Disaster Reduction in Civil Engineering, Tongji University, China

<sup>2</sup> State Key Laboratory of Disaster Reduction in Civil Engineering, Tongji University, China

<sup>3</sup> Department of Civil & Structural Engineering, Hong Kong Polytechnic University, China

<sup>4</sup> State Key Laboratory of Disaster Reduction in Civil Engineering, Tongji University, China

<sup>5</sup> Jiangsu Wanbao Bridge Component Co., Ltd., China

---

### Abstract

This paper reports on the study of the performance of a new seismic control device named as cable-sliding friction aseismic bearing (CSFAB), which combines a conventional aseismic bearing with restrainer cables to dissipate earthquake energy and at the same time to control the displacement of girder to an acceptable value. A two-dimensional long-span continuous girder bridge model was developed and analyzed in the study. Considering the influence of different site conditions, the model was subjected to three historic ground motion records applied to different (A,B,C,D) site conditions specified in the USGS site classification. Compared with conventional aseismic bearing, the effectiveness of the CSFAB in controlling the girder displacement and limiting the shear force and bending moment demands on the bridge piers was assessed. Furthermore, study considering different fixed pier heights was conducted and the results showed that with the decrease of height or increase in stiffness of piers, CSFAB was to be more effective.

© 2011 Published by Elsevier Ltd. Open access under [CC BY-NC-ND license](https://creativecommons.org/licenses/by-nc-nd/4.0/).

**Keywords:** cable-sliding friction aseismic bearing; continuous girder bridge; seismic isolation; hysteresis curve; restoring force model.

---

<sup>a</sup> Corresponding author: Email: [wzhyicheng@gmail.com](mailto:wzhyicheng@gmail.com)

<sup>b</sup> Presenter: Email: [wzhyicheng@gmail.com](mailto:wzhyicheng@gmail.com)

## 1. INTRODUCTION

Continuous girder bridges which are well-known for their versatility in meeting different requirements such as long span but practically shallow depth, and varying forms, constitute a major part of country's highway and railway systems. A large number of studies aimed at studying the dynamic behavior of continuous girder bridges under extreme dynamic loads such as earthquakes have revealed their vulnerability to collapse due to a chain of element failures. These studies have shown that although restraining the bridge girder completely at the pier locations could limit the girder displacement, it would cause a significant increase in the demands on the piers in terms of bending moments and shear forces. Therefore, many researchers have suggested that the main girder should not be fixed to the piers, but instead be allowed to experience some relative movement at these locations, which would lead to a reduction in the overall forces transmitted from the girder to the piers (Sharabash and Andrawes 2009).

In order for this design approach to be implemented successfully, the use of restrainer cables and restrainer bars located between the girder and piers of bridges become popular following the collapse of several bridges in recent earthquakes (DesRoches and Delemont 2002), but these devices inevitably need additional design of girder and piers, increasing construction cost. Meanwhile, in the last two decades a large number of studies have focused on developing effective and reliable dynamic control devices for continuous girder bridges. The most basic device that has been studied extensively is laminated rubber bearing, which would respond linearly under seismic horizontal forces (Priestley et al 1996; Yang et al. 2008). Although this class of devices is simple and cost-effective, it has a poor stability and is only used in small bridges. Another type of device that has been studied and used in the past is metallic damper (Sharabash and Andrawes 2009) which provides energy dissipation through plastic deformation, but needs to be replaced after a severe earthquake, resulting in high cost repair. Among those aseismic devices that have been either studied or applied in more recent years are lead rubber bearings whose hysteresis curves show bilinear characteristics and extensive energy dissipation, but with the increase of the lead material, the self-recovery capability of rubber bearing deteriorates gradually (Priestley et al 1996; Ye 2002). The previous studies illustrate that there is still a need for further improvement in the field of dynamic control of bridges. This study presents a new class of bearing named as cable-sliding friction aseismic bearing (CSFAB) that could overcome many of the shortcomings previously discussed, and its unique characteristics are presented in the following sections.

## 2. OVERVIEW OF CSFAB

CSFAB is the combination of ordinary aseismic bearing and restrainer cables, and thus can be categorized according to the types of aseismic bearing and cable materials it adopts, such as the combination of spherical steel bearing and high strength steel tendon or carbon fiber. CSFAB studied in this article is the combination of pot rubber bearing and strands. The configuration of a fixed bearing is shown in Fig.1.

While setting on the fixed pier of a continuous bridge, CSFAB ensures the bearing keep fixed in normal conditions by the effect of shear bolt and the horizontal loads are mainly transmitted to the fixed pier. In extreme loading conditions such as a severe earthquake, ship-impact, or explosion, etc. the shear bolt is sheared off as the horizontal loads exceed a certain value. As a result, the bearing is changed into a sliding one, which alters the characteristics of load transfer mechanism of the system and distributes the horizontal loads to all piers. Compared with normal conditions, girder displacement in this case inevitably becomes larger, but the cables of the bearing begin to work as a buffer and displacement-restrainer which can limit the excessive displacement.

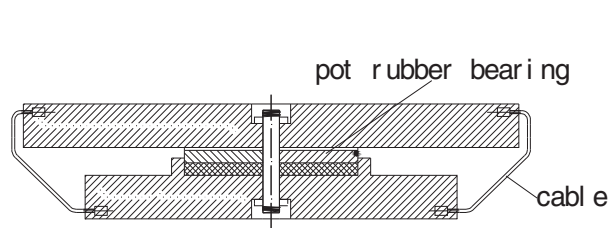


Fig.1 Configuration of fixed CSFAB

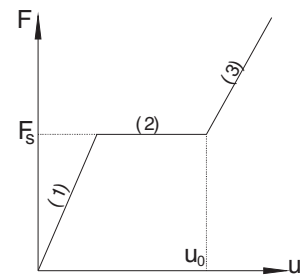


Fig.2 Restoring force model

An important task of this study is to design the CSFAB to limit the excessive displacement. An ideal restoring model developed in this article can be divided into three phases, as shown in Fig.2: (1) energy dissipation phase; (2) transformation phase which is characterized by a very low modulus and thus resembles yielding in materials with typical plastic behavior; (3) displacement-limiting phase, in which cables provide a large longitudinal stiffness to limit the excessive relative displacement between the superstructure and the substructure.  $F_s$  and  $u_0$  are defined as the critical friction force and displacement respectively, and cables work only when the relative displacement between the girder and piers exceeds  $u_0$ . Using the restoring force model, a former study has shown that it is feasible to simulate CSFAB behavior using finite element modeling (Cao 2009).

### 3. CASE STUDY

Excessive relative displacement of multi-span continuous girder bridges between upper girder and lower piers can result in collapse of the bridge in a chain. However, CSFAB can be designed to provide sufficient stiffness to limit the relative displacement below a pre-determined value, and thus serve as a more effective alternative to conventional aseismic bearings. A multi-span continuous bridge considered in this paper consists of four spans (55m+2×85m+78m) and is based on the north approach bridge of Jiubao Bridge in Hangzhou city. The upper composite box girder is supported on the top of single box piers, and section properties are listed in Table 1. The piers are fixed at the bottom as the effect of soil-structure interaction is ignored. The calculation model of whole bridge is shown in Fig.3.

Table 1 Section properties

|        | Area(m <sup>2</sup> ) | Moment of inertial(m <sup>4</sup> ) |
|--------|-----------------------|-------------------------------------|
| Girder | 2.054                 | 120.70                              |
| Pier   | 15.91                 | 179.43                              |

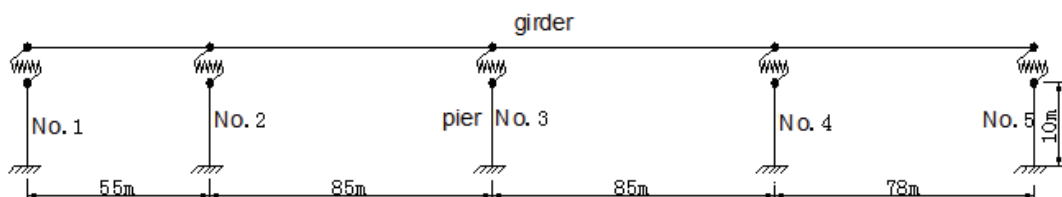


Fig.3 Calculation model of case study

A 2-D finite element model of the reference bridge is developed and analyzed using SAP2000 finite element software program. In order to define the retrofit effectiveness of CSFAB, the following two cases are considered:

- ① A fixed pot rubber bearing is set at the top of No.3 pier (fixed pier), and sliding ones are set at the top of other piers (sliding piers).
- ② A fixed CSFAB is set at the top of No.3 pier, and sliding ones are set at the top of other piers. However, as designed, the shear bolt of fixed CSFAB will be sheared off in a severe earthquake, thus changing the fixed bearing into a sliding one.

In finite element models, pot rubber bearings and elastic cables are simulated using wen-plastic link element and multilinear elastic link element respectively (Yan et al. 2009). Critical displacement  $u_0$  is 6cm, friction coefficient adopted is 2%, and cable stiffness is  $1.0 \times 10^6 \text{ kN/m}$ .

### 3.1 Influence of site condition

To evaluate the effectiveness of CSFAB on different site conditions, the bridge is subjected to three earthquake ground motion records applied to different A,B,C,D site condition specified in USGS site classification, as shown in Table 2. In this paper, acceleration peaks are adjusted to 0.4g uniformly. The input earthquake waves in horizontal and vertical directions which can be achieved by multiplying an adjustment coefficient to the corresponding horizontal seismic waves, and a damping ratio of 5% are adopted. The time history analysis results in the two cases are listed in Table 3 to Table 4 and Fig.4.

Table 2 Selected earthquake motion records

| Site condition | No. | earthquake wave records | site               | magnitude | PGA/g |
|----------------|-----|-------------------------|--------------------|-----------|-------|
| A              | 1   | 1989 LOMA PRIETA        | Gilroy Array 1#    | 7.1       | 0.209 |
|                | 2   | 1999 CHI-CHI            | HWA                | 7.3       | 0.107 |
|                | 3   | 1992 LANDERS            | Amboy              | 7.3       | 0.146 |
| B              | 4   | 1979 IMPERIAL VALLEY    | El Centro allay 4# | 6.5       | 0.157 |
|                | 5   | 1992 LANDERS            | Coolwater          | 7.3       | 0.417 |
|                | 6   | 1989 LOMA PRIETA        | Anderson Dam       | 6.9       | 0.240 |
| C              | 7   | 1999 CHI-CHI            | CHY006             | 7.3       | 0.364 |
|                | 8   | 1979 IMPERIAL VALLEY    | El Centro allay 5# | 6.5       | 0.537 |
|                | 9   | 1992 LANDERS            | YermoFire Station  | 7.3       | 0.152 |
| D              | 10  | 1979 IMPERIAL VALLEY    | Agrarias           | 6.5       | 0.221 |
|                | 11  | 1999 CHI-CHI            | CHY039             | 7.3       | 0.114 |
|                | 12  | 1989 LOMA PRIETA        | Redwood City       | 6.9       | 0.083 |

From Table 3, it can be concluded that the maximum displacements at the end of girder along the bridge in case② are larger than the ones in case①, because the shear bolt of fixed bearing in case② will be broken in a severe earthquake, making the longitudinal constraint of girder weaker than that of case①. However, the maximum displacements at the top of piers in case② are smaller than the ones in case①, as seismic forces transmitted from girder to piers are smaller than that of case①.

Table 3 Maximum displacements along the bridge

|        |           | 1   | 2   | 3   | 4    | 5   | 6   | 7   | 8   | 9    | 10  | 11   | 12   |
|--------|-----------|-----|-----|-----|------|-----|-----|-----|-----|------|-----|------|------|
| Girder | case①/cm  | 2.9 | 3.8 | 5.0 | 7.6  | 8   | 6.5 | 8.8 | 1.8 | 2.4  | 5.1 | 9.2  | 4.5  |
|        | case②/cm  | 7.7 | 8.1 | 11  | 10.8 | 9.7 | 7.6 | 9.9 | 7.7 | 10.2 | 9   | 13.2 | 10.2 |
|        | (②-①)/①/% | 166 | 113 | 120 | 42   | 21  | 17  | 13  | 328 | 325  | 77  | 44   | 127  |
| Pier   | case①/cm  | 2.4 | 3.2 | 4.1 | 6.2  | 6.8 | 5.5 | 7.6 | 1.5 | 1.9  | 4.2 | 7.9  | 3.6  |
|        | case②/cm  | 0.5 | 0.6 | 1.8 | 1.7  | 1   | 0.5 | 1.2 | 0.3 | 1.4  | 1   | 2.8  | 1.6  |
|        | (②-①)/①/% | -79 | -81 | -56 | -73  | -85 | -91 | -84 | -80 | -26  | -76 | -65  | -56  |

Table 4 Moment/shear force at the bottom of piers

|    | Sliding pier   |               |           | Fixed pier      |               |          |
|----|----------------|---------------|-----------|-----------------|---------------|----------|
|    | case (kN.m/kN) | case(kN.m/kN) | (-)/ (%)  | case (kN.m/kN)  | case(kN.m/kN) | (-)/ (%) |
| 1  | 9408/1556      | 48068/5055    | 411/225   | 678436/37087    | 67875/7073    | -90/81   |
| 2  | 9453/1570      | 84402/8572    | 793/446   | 516700/51066    | 96137/9771    | -81/81   |
| 3  | 8519/1440      | 253308/26204  | 2873/1720 | 652366/64629    | 282985/29376  | -57/55   |
| 4  | 9209/1520      | 233980/24048  | 2441/1482 | 998889/98903    | 259623/26584  | -74/73   |
| 5  | 8647/1465      | 160661/16192  | 1758/1005 | 1.09E+06/108342 | 151911/15251  | -86/86   |
| 6  | 9257/1547      | 31141/3165    | 236/105   | 885637/87762    | 82232/8390    | -91/90   |
| 7  | 8663/1468      | 168482/17371  | 1845/1083 | 1.23E+06/121577 | 180588/18611  | -85/85   |
| 8  | 9138/1415      | 51789/5583    | 467/295   | 240016/23561    | 56398/6064    | -77/74   |
| 9  | 9701/1589      | 203588/21028  | 1999/1223 | 313630/31160    | 226102/23379  | -28/25   |
| 10 | 7254/4339      | 140866/14287  | 1842/229  | 682900/67420    | 167688/17144  | -75/75   |
| 11 | 8593/1455      | 407911/42095  | 4647/2793 | 1.27E+06/126294 | 434909/44837  | -66/65   |
| 12 | 8737/1476      | 216432/22382  | 2377/1416 | 582227/57464    | 247032/25311  | -58/56   |

The seismic responses of fixed pier (No.3 pier) and sliding pier (taking No.1 pier for example) are listed in Table 4. It can be concluded that bending moments and shear forces at the bottom of fixed pier in case ② are smaller than the ones in case①, because the shear bolt of the fixed bearing will be cut off in case② in a severe earthquake, and the horizontal seismic forces transmitted from girder to the fixed pier initially are taken on by all piers, minimizing the forces taken by the fixed pier accordingly. In Table 4, the maximum reduction of bending moment at the bottom of the fixed pier is -91%, and the maximum reduction of shear force at the bottom of fixed pier is -90%. Compared with the fixed pier, bending

moments and shear forces at the bottom of sliding pier in case② are larger than the ones in case①, because the forces transmitted from the girder to other sliding piers in case② are larger than those in case①, but still smaller than the forces transmitted to the fixed pier in case①.

It is also shown in Table 4 that the forces transmitted from girder to piers in case② are more balanced than those in case①, but as design, all piers have uniform section properties, which means that retrofit ability of each pier is exploited more fully in case② than that in case①, and all piers unit to resist the earthquake force.

Furthermore, it both reveals the well adaptation to the different site condition of CSFAB in Table 4, as there is a similar trend as above for each site condition.

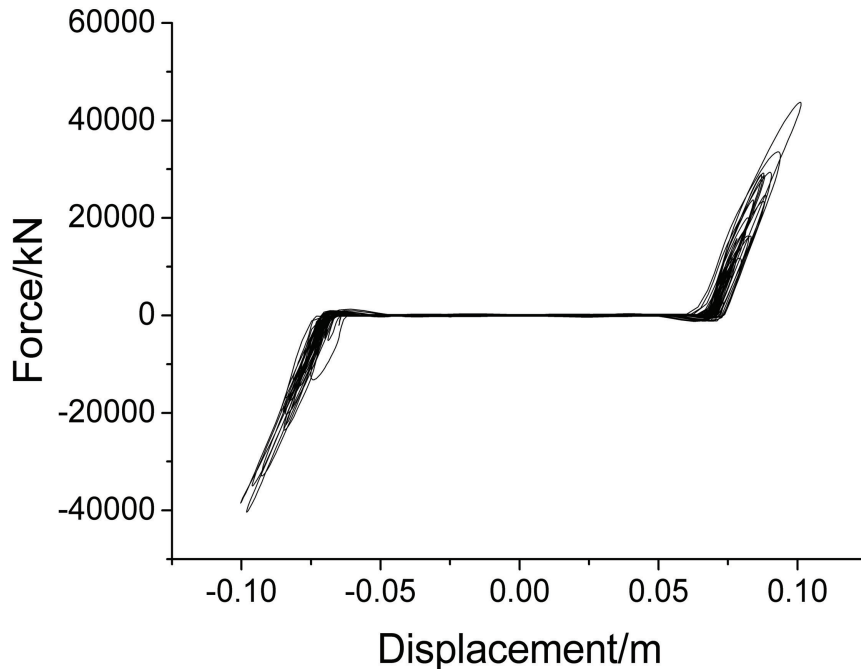


Fig.4 Force deformation relationship of CSFAB for bridge subjected to No.11 record

It is shown in Fig.4 that the typical force displacement relationship of CSFAB in the case of No.11 record loading (1999 chi-chi) matches ideal restoring force model in Fig.2 well. The maximum displacement of CSFAB in Fig.4 is limited below 0.10m, providing a practical solution for preventing girder falling caused by excessive displacement.

### 3.2 Influence of pier height change

To evaluate the effectiveness of CSFAB to different pier height, four finite element models with different fixed pier height of 10m,15m, 20m, and 25m respectively in case② are established, and earthquake ground motion records adopted in this section are also same to those in Table 2. The results are shown in Table 5 to Table 7.

Table 5 Maximum displacements of girder with different pier height (unit: cm)

| Wave Height/m \ | 1   | 2   | 3    | 4    | 5    | 6   | 7    | 8   | 9    | 10  | 11   | 12   |
|-----------------|-----|-----|------|------|------|-----|------|-----|------|-----|------|------|
| 10              | 7.7 | 8.1 | 11   | 10.8 | 9.7  | 7.6 | 9.9  | 7.7 | 10.2 | 9   | 13.2 | 10.2 |
| 15              | 7.6 | 8.1 | 11   | 12.6 | 10.6 | 7.7 | 10   | 7.7 | 9.8  | 9.1 | 12.1 | 10.6 |
| 20              | 7.8 | 7.7 | 10.3 | 11.4 | 10.9 | 7.8 | 10.1 | 7.8 | 9.9  | 9.1 | 14   | 10.7 |
| 25              | 7.9 | 8.4 | 10.9 | 13.1 | 11.7 | 7.7 | 10.1 | 7.8 | 10   | 9.3 | 13.2 | 10.5 |

Table 6 Maximum moments at the bottom of piers with different pier height (unit: kN.m)

| Wave Height/m \ | 1     | 2      | 3      | 4      | 5      | 6     | 7      | 8     | 9      | 10     | 11     | 12     |
|-----------------|-------|--------|--------|--------|--------|-------|--------|-------|--------|--------|--------|--------|
| 10              | 64518 | 97681  | 282985 | 275515 | 169927 | 78450 | 199004 | 59889 | 234749 | 167688 | 455945 | 255518 |
| 15              | 85664 | 82657  | 285831 | 414130 | 252763 | 83226 | 206088 | 61520 | 202834 | 170317 | 364912 | 270875 |
| 20              | 94523 | 65563  | 231584 | 324805 | 255745 | 84810 | 210244 | 59166 | 208682 | 172050 | 500865 | 261627 |
| 25              | 88659 | 123773 | 279179 | 427924 | 356646 | 79780 | 208434 | 62664 | 211159 | 178862 | 422881 | 261890 |

It can be concluded from Table 5 and Table 6 that with the increase of pier height, structure responses are increased accordingly. For example, the maximum structure response increases with the different height of 10m and 25m are listed in Table 7.

Table 7 Comparison of responses of different pier height conditions

| Height   | Maximum displacement/cm | Maximum moment/kN.m |
|----------|-------------------------|---------------------|
| 10m      | 10.8                    | 169927              |
| 25m      | 13.1                    | 356646              |
| Increase | 21%                     | 110%                |

It is shown in Table 7 that with the increase of pier height, the maximum displacements at the end of girder along the bridge increase marginally, but bending moments and shear forces both show a significant increasing trend, indicating that the shorter and stiffer the pier is, the more effective CSFAB retrofit is.

#### 4. CONCLUSION

This paper presents an analytical study on the feasibility of using a new class of aseismic bearing——CSFAB for the seismic control of continuous girder bridges. A 2-D continuous bridge model is developed and utilized in the study. The model is subjected to two orthogonal components of three historic earthquake motion records for each site condition respectively. The seismic behavior of a CSFAB-

controlled bridge is compared with the behavior of an identical bridge controlled by ordinary aseismic bearing, and it indicates a more retrofit effectiveness of CSFAB, key findings are summarized below:

- (1) CSFAB shows a well adaptation to different site conditions, and all piers unit to resist the earthquake force.
- (2) The displacements of both girder and pier can be limited below a pre-determined value, and thus CSFAB serves as a more effective alternative to conventional aseismic bearings;
- (3) A further study considering the influence of pier height to the effectiveness of CSFAB reveals that CSFAB can achieve the aims of limiting displacement, and the shorter and stiffer the pier, the more effective the CSFAB retrofit is.

## 5. ACKNOWLEDGEMENTS

This research is supported by Ministry of Science and Technology of China, Grant No. SLDRCE 09-B-08, and the National Science Foundation of China, Grants No.50778131, No.50978194 and No.90915011.

## REFERENCES

- [1] Sharabash Alaa M., and Andrawes Bassem O. (2009). Application of shape memory alloy dampers in the seismic control of cable-stayed bridges. *Engineering Structures*.31.pp.607-616
- [2] DesRoches, R., and Delemont, M. (2002). Seismic retrofit of simply supported bridges using shape memory alloys. *Engineering Structures*,24.pp.325-332
- [3] Priestley M J N, Seible F. and Calvi G M(1996). *Seismic design and retrofit of bridges*. John Wiley & Sons.Inc.
- [4] Yang Yan-fei, Wang Xitang, and Chen Wen-chun(2008).Bridge bearings and restoring force model. *Guangzhou Architecture*. 36(6).pp.11-15
- [5] Ye Aijun(2002). *Seismic design of bridge*. China Communication Press.
- [6] Cao Xinjian (2009). Design strategy on aseismic capacity of large bridge. Ph. D. thesis, Department of Bridge Engineering, Tongji University.
- [7] Yan Dong, Qi Chunxiang, and Feng Qinghai(2009). *SAP2000 structural engineering analysis and examples explanation*. China Architecture & Building Press.